An integrative description of a population of *Mesobiotus radiatus* (Pilato, Binda & Catanzaro, 1991) from Kenya

Daniel STEC[1,]* , Milena ROSZKOWSKA[2,3] , Łukasz KACZMAREK[2] , Łukasz MICHALCZYK[1]

[1]Institute of Zoology and Biomedical Research, Jagiellonian University, Kraków, Poland
[2]Department of Animal Taxonomy and Ecology, Faculty of Biology, Adam Mickiewicz University in Poznań, Poznań, Poland
[3]Department of Bioenergetics, Faculty of Biology, Adam Mickiewicz University in Poznań, Poznań, Poland

Abstract: In a moss sample collected from Mount Kulal in Kenya, a new population of *Mesobiotus radiatus* was found. Given that the original description of *M. radiatus* was based solely on the morphology observed by light microscopy and measurements based mostly on a single individual, here we describe the new population by means of integrative taxonomy and a large sample size. We provide an integrative description comprising a comprehensive set of morphometric and morphological data from light and scanning microscopy as well as nucleotide sequences of three nuclear fragments (18S rRNA, 28S rRNA, ITS-2) and one mitochondrial fragment (COI). *Mesobiotus radiatus* is most similar to *M. binieki*, *M. coronatus*, *M. patiens*, *M. perfidus*, *M. philippinicus*, *M. pseudocoronatus*, *M. pseudopatiens*, *M. rigidus*, *M. simulans*, and *M. wuzhishanensis*, but differs from them mainly by egg morphology and morphometry, and some characters of adult specimens.

Key words: Africa, 18S rRNA, 28S rRNA, COI, ITS-2, *Mesobiotus harmsworthi* group, integrative taxonomy

1. Introduction

Tardigrades are a phylum of small invertebrates inhabiting terrestrial and aquatic, both freshwater and marine, habitats (Nelson et al., 2015). To date over 1200 species have been described, and every year over a dozen of species new to science are discovered (Guidetti and Bertolani, 2005; Degma and Guidetti, 2007; Degma et al., 2009-2018).

The Kenyan tardigrade fauna is still poorly known as until now only 27 species have been reported from this sub-Saharan country (McInnes et al., 2017). Moreover, only four of them have type localities in this country: *Minibiotus allani* (Murray, 1913); *Paramacrobiotus* (*P.*) *kenianus* Schill, Förster, Dandekar & Wolf, 2010; *Doryphoribius maasaimarensis* Fontoura, Lisi & Pilato, 2013; and *Macrobiotus paulinae* Stec, Smolak, Kaczmarek & Michalczyk, 2015. The last three have not been found outside Kenya, whereas the first one was reported from a few disjunct localities (see McInnes, 1994 and McInnes et al., 2017). Despite the fact that the family Macrobiotidae in Kenya is represented by three cosmopolitan tardigrade genera (*Paramacrobiotus* Guidetti, Schill, Bertolani, Dandekar & Wolf, 2009; *Macrobiotus* C.A.S. Schultze, 1834; and *Minibiotus* R.O. Schuster, 1980), the fourth widely distributed genus,

Mesobiotus Vecchi, Cesari, Bertolani, Jönsson, Rebecchi & Guidetti, 2016, has never been reported from this country (McInnes et al., 2017).

Mesobiotus radiatus (Pilato, Binda & Catanzaro, 1991) is an African tardigrade of the *Mesobiotus harmsworthi* group, originally described from the Ngorongoro District in Tanzania and reported a decade later also from two localities in North Kivu Province in the Democratic Republic of Congo by Binda et al. (2001). The original description of this species is still valid; however, it was prepared prior to the integrative taxonomy era and thus the description was based solely on morphology and morphometry. The morphology was documented by the description per se and by drawings based on light microscopy. Moreover, measurements were based mostly on a single individual and thus intraspecific variability was not described. In order to fill these gaps and to provide more detailed data that may be needed for future species discovery and identification, we integratively (Dayrat, 2005) describe a new population of *M. radiatus* found in Kenya. Our work involved an integrative taxonomy approach that comprised morphological and morphometric data obtained with phase contrast light microscopy (PCM) and scanning electron microscopy (SEM) as well as molecular

* Correspondence: daniel_stec@interia.eu

523

data in the form of DNA sequences of four molecular markers (three nuclear: 18S rRNA, 28S rRNA, ITS-2; one mitochondrial: COI).

2. Materials and methods

2.1. Sample processing
A moss sample from soil from Mount Kulal (Kenya, Africa) was collected by Maciej Skoracki on 25 January 2014. The sample was examined for terrestrial tardigrades using standard methods (Dastych, 1980) with modifications by Stec et al. (2015). Together with *Mesobiotus radiatus*, representatives of three other tardigrade genera were found: *Echiniscus* C.A.S. Schultze, 1840; *Milnesium* Doyère, 1840; and *Macrobiotus* C.A.S. Schultze, 1834. A total of 25 live individuals and four eggs of *M. radiatus* were extracted from the sample. Eggs were mounted on slides and animals were placed in a culture in order to obtain more individuals and eggs for further analyses. All 25 specimens were placed and reared on plastic petri dishes according to the protocol of Stec et al. (2015). In order to perform the taxonomic analysis of this species, animals and eggs were taken from the culture and split into groups: 94 animals and 102 eggs were mounted on microscope slides in Hoyer's medium; 20 animals and 15 eggs were prepared for SEM imaging; four specimens were processed for DNA extraction and sequencing (see below for details); and 20 specimens were used for aceto-orcein staining.

2.2. Species identification
The population that is the subject of this study fits the original description of *M. radiatus* well. However, to corroborate our identification, we compared our tardigrades to photomicrographs of a type specimen that were kindly sent to us by Professor Giovanni Pilato, one of the authors of the original description of *M. radiatus*.

2.3. Microscopy and imaging
Specimens for light microscopy were prepared according to the protocol of Morek et al. (2016). Microscopic slides were examined under a Nikon Eclipse 50i phase contrast light microscope associated with a Nikon Digital Sight DS-L2 digital camera. Animals and eggs for SEM were processed according to the protocol of Stec et al. (2015). Buccopharyngeal apparatuses were extracted following the protocol of Eibye-Jacobsen (2001) with modifications by Gąsiorek et al. (2016). Dried animals, eggs, and buccal apparatuses were examined under high vacuum with a Versa 3D DualBeam scanning electron microscope at the ATOMIN facility of Jagiellonian University, Kraków, Poland. The type population was also examined for the presence of males with aceto-orcein staining in accordance with Stec et al. (2016b).

All figures were assembled in Corel Photo-Paint X6, ver. 16.4.1.1281. For structures that could not be satisfactorily focused in a single photograph, a stack of 2–6 images were taken with an equidistance of ca. 0.2 µm and assembled manually into a single deep-focus image.

2.4. Morphometrics and morphological nomenclature
The sample size for morphometrics was chosen following the recommendations of Stec et al. (2016a). All measurements are given in micrometers (µm). Structures were measured only if their orientation was suitable. Body length was measured from the anterior extremity to the end of the body, excluding the hind legs. The buccal apparatus and claw types are given according to Pilato and Binda (2010). The terminology used to describe oral cavity armature follows that of Michalczyk and Kaczmarek (2003). Buccal tube length and the level of the stylet support insertion point were measured according to Pilato (1981). Claws were measured according to Kaczmarek and Michalczyk (2017). Macroplacoid length sequence is given according to Kaczmarek et al. (2014). The *pt* index is the ratio of the length of a given structure to the length of the buccal tube expressed as a percentage (Pilato, 1981). Distance between egg processes was measured as the shortest line connecting base edges of the two closest processes (Kaczmarek and Michalczyk, 2017). The description of claw morphology follows Vecchi et al. (2016). Morphometric data were handled using the Parachela ver. 1.3 template available from the Tardigrada Register (Michalczyk and Kaczmarek, 2013). Tardigrade taxonomy follows Bertolani et al. (2014).

2.5. Genotyping
The DNA was extracted from individual animals following the Chelex 100 resin (Bio-Rad) extraction method of Casquet et al. (2012) with modifications described in detail by Stec et al. (2015). Four DNA fragments have been sequenced: 18S rRNA, 28S rRNA, ITS-2, and COI. All fragments were amplified and sequenced according to the protocols described by Stec et al. (2015); primers and original references for specific PCR programs are listed in Table 1. Sequencing products were read with the ABI 3130xl sequencer at the Molecular Ecology Lab, Institute of Environmental Sciences of Jagiellonian University, Kraków, Poland. Sequences were processed in BioEdit ver. 7.2.5 (Hall, 1999). The DNA sequences are deposited in GenBank (https://www.ncbi.nlm.nih.gov/genbank).

2.6. Comparative molecular analysis
For molecular comparisons, all published sequences of the four abovementioned markers for species of the genus *Mesobiotus* were downloaded from GenBank (listed in Table 2). The sequences were aligned using the default settings (mitochondrial marker) and the Q-INS-I method (nuclear markers) of MAFFT version 7 (Katoh et al., 2002; Katoh and Toh, 2008) and manually checked against nonconservative alignments in BioEdit. Then the aligned sequences were trimmed to 739 (18S rRNA), 736 (28S

Table 1. Primers and references for PCR protocols for amplification of the four DNA fragments sequenced in the study.

DNA fragment	Primer name	Primer direction	Primer sequence (5'-3')	Primer source	PCR program
18S rRNA	18S_Tar_Ff1	Forward	AGGCGAAACCGCGAATGGCTC	Stec et al. (2017)	Zeller (2010)
	18S_Tar_Rr2	Reverse	CTGATCGCCTTCGAACCTCTAACTTTCG	Gąsiorek et al. (2017)	
28S rRNA	28SF0001	Forward	ACCCVCYNAATTTAAGCATAT	Mironov et al. (2012)	Mironov et al. (2012)
	28SR0990	Reverse	CCTTGGTCCGTGTTTCAAGAC		
ITS-2	ITS2_Eutar_Ff	Forward	CGTAACGTGAATTGCAGGAC	Stec et al. (2018)	Stec et al. (2018)
	ITS2_Eutar_Rr	Reverse	TCCTCCGCTTATTGATATGC		
COI	LCO1490	Forward	GGTCAACAAATCATAAAGATATTGG	Folmer et al. (1994)	Michalczyk et al. (2012)
	HCO2198	Reverse	TAAACTTCAGGGTGACCAAAAAATCA		

Table 2. Sequences used for molecular comparisons and phylogenetic analyses of *Mesobiotus radiatus* (Pilato, Binda & Catanzaro, 1991) from Kenya with all other species of the genus *Mesobiotus* for which DNA sequences are currently available and suitable for fragments amplified in this study. The 18S rRNA sequence of *M. insanis* has not been used due to its short length.

DNA marker	Species	Accession number	Source
18S rRNA	*M. ethiopicus* Stec & Kristensen, 2017	MF678793	Stec and Kristensen (2017)
	M. philippinicus Mapalo et al., 2016	KX129793	Mapalo et al. (2016)
	M. hilariae Vecchi et al., 2016	KT226068–71	Vecchi et al. (2016)
	M. polaris (Murray, 1910)	KT226075–8	Vecchi et al. (2016)
	M. cf. *mottai*	KT226072	Vecchi et al. (2016)
	M. harmsworthi group species	KT226073–4	Vecchi et al. (2016)
	M. harmsworthi group species	HQ604967–70	Bertolani et al. (2014)
28S rRNA	*M. ethiopicus* Stec & Kristensen, 2017	MF678792	Stec and Kristensen (2017)
	M. philippinicus Mapalo et al., 2016	KX129794	Mapalo et al. (2016)
	M. insanis Mapalo et al., 2017	MF441489	Mapalo et al. (2017)
ITS-2	*M. philippinicus* Mapalo et al., 2016	KX129795	Mapalo et al. (2016)
	M. insanis Mapalo et al., 2017	MF441490	Mapalo et al. (2017)
COI	*M. ethiopicus* Stec & Kristensen, 2017	MF678794	Stec and Kristensen (2017)
	M. philippinicus Mapalo et al., 2016	KX129796	Mapalo et al. (2016)
	M. insanis Mapalo et al., 2017	MF441491	Mapalo et al. (2017)
	M. hilariae Vecchi et al., 2016	KT226108	Vecchi et al. (2016)

rRNA), 363 (ITS-2), and 636 (COI) bp. The COI sequences were translated into protein sequences in MEGA7 version 7.0 (Kumar et al., 2016) to be checked against pseudogenes. Uncorrected pairwise distances were calculated using MEGA. Despite genetic distances in barcoding studies frequently being calculated in accordance with the Kimura 2 parameter model (K2P), as proposed by Hebert et al. (2003), the more recent work by Srivathsan and Meier (2012) showed that this model of nucleotide evolution is poorly justified. Moreover, Srivathsan and Meier

(2012) showed that uncorrected p-distances may provide a comparable or even a higher success rate of taxon delimitation than distances computed under the K2P. Therefore, we used basic p-distances in all of our analyses.

3. Results

3.1. Taxonomic account of the studied species
Phylum: Tardigrada Doyère, 1840
Class: Eutardigrada Richters, 1926
Order: Parachela Schuster, Nelson, Grigarick &

Christenberry, 1980
   Superfamily: Macrobiotoidea Thulin, 1928 (in Marley et al., 2011)
   Family: Macrobiotidae Thulin, 1928

Genus: *Mesobiotus* Vecchi, Cesari, Bertolani, Jönsson, Rebecchi & Guidetti, 2016
   Mesobiotus radiatus (Pilato, Binda & Catanzaro, 1991)
   (Tables 2 and 3, Figures 1–10)

Table 3. Measurements [in µm] of selected morphological structures of individuals of *Mesobiotus radiatus* (Pilato, Binda & Catanzaro, 1991) from Kenya mounted in Hoyer's medium (N: number of specimens/structures measured, Range: the smallest and the largest structures among all measured specimens; SD: standard deviation).

Character	N	Range		Mean		SD	
		µm	*pt*	µm	*pt*	µm	*pt*
Body length	30	370–798	*979–1425*	520	*1198*	104	*127*
Buccopharyngeal tube							
Buccal tube length	30	35.6–56.0	–	43.1	–	4.8	–
Stylet support insertion point	30	27.6–44.4	*74.0–79.6*	33.2	*77.0*	3.9	*1.4*
Buccal tube external width	30	5.0–10.2	*12.9–19.3*	7.0	*16.1*	1.2	*1.3*
Buccal tube internal width	30	3.9–8.4	*10.1–15.0*	5.4	*12.4*	1.0	*1.2*
Ventral lamina length	26	21.8–36.5	*54.5–65.3*	26.6	*61.3*	3.5	*2.5*
Placoid lengths							
Macroplacoid 1	30	4.9–9.7	*12.7–19.1*	6.9	*16.0*	1.3	*1.6*
Macroplacoid 2	30	3.8–7.4	*10.1–16.1*	5.4	*12.6*	1.0	*1.5*
Macroplacoid 3	30	4.3–11.8	*12.1–23.5*	7.0	*16.0*	1.7	*2.4*
Microplacoid	29	3.7–6.2	*8.9–14.2*	4.9	*11.3*	0.8	*1.5*
Macroplacoid row	30	16.8–30.6	*39.7–61.0*	22.3	*51.6*	3.7	*4.4*
Placoid row	29	21.1–38.5	*54.5–77.2*	28.3	*65.8*	4.5	*4.8*
Claw 1 lengths							
External primary branch	25	11.1–17.0	*28.7–42.6*	13.9	*32.6*	1.7	*3.1*
External secondary branch	22	7.3–13.9	*19.5–28.8*	10.2	*23.6*	1.5	*2.5*
Internal primary branch	24	8.6–15.7	*23.1–32.4*	11.6	*26.9*	1.7	*2.4*
Internal secondary branch	11	8.2–10.9	*16.6–25.9*	9.1	*21.4*	0.8	*2.7*
Claw 2 lengths							
External primary branch	27	10.3–20.1	*26.6–39.3*	14.6	*33.7*	2.1	*3.0*
External secondary branch	21	8.1–13.4	*21.4–28.4*	10.4	*24.7*	1.4	*1.7*
Internal primary branch	27	8.3–14.6	*23.3–33.9*	11.8	*27.6*	1.5	*2.4*
Internal secondary branch	17	6.3–11.3	*16.3–25.3*	9.4	*21.9*	1.3	*2.4*
Claw 3 lengths							
External primary branch	28	10.3–20.1	*28.9–41.5*	14.9	*34.7*	2.1	*3.2*
External secondary branch	21	8.8–13.8	*22.0–28.0*	10.7	*25.2*	1.1	*1.9*
Internal primary branch	23	9.5–14.5	*23.3–32.4*	11.8	*27.4*	1.4	*2.6*
Internal secondary branch	17	6.7–11.4	*17.3–25.9*	9.2	*21.6*	1.3	*2.5*
Claw 4 lengths							
Anterior primary branch	27	10.2–18.0	*28.7–40.2*	14.7	*34.0*	1.9	*2.4*
Anterior secondary branch	20	8.4–13.3	*20.4–29.4*	11.1	*25.6*	1.2	*2.3*
Posterior primary branch	28	12.0–20.8	*31.0–42.6*	15.9	*36.9*	2.0	*2.6*
Posterior secondary branch	15	9.8–13.4	*23.9–30.6*	11.5	*27.6*	1.0	*1.9*

3.2. Material examined

A total of 138 animals (including 6 simplex) and 117 eggs were studied. Specimens were mounted on microscope slides in Hoyer's medium (94 animals + 102 eggs), fixed on SEM stubs (20 + 15), or processed for DNA sequencing (4 + 0) and aceto-orcein staining (20 + 0).

3.3. Population locality

Locality: 2°39′15.75″N, 36°56′9.99″E; 1824 m a.s.l.: Kenya, Eastern Province, Marsabit County, Mount Kulal Biosphere Reserve, Kulal Mt., near Gatab. Habitat: Compact high, dense, and shady forest (with approximately 30 min of sunshine a day reaching the forest floor), coll. Maciej Skoracki.

3.4. Depositories

Twenty-eight animals (slides: KE.008.*, where the asterisk can be substituted by any of the following numbers: 7–24, 26–28), 44 eggs (slides: KE.008.*: 1–6, 25, 40), and all SEM stubs are deposited at the Institute of Zoology and Biomedical Research, Jagiellonian University, Kraków, Poland. Sixty-six animals (slides: KE.008.*: 42–48, 57–60) and 58 eggs (slides: KE.008.*: 49–56) are deposited in the Department of Animal Taxonomy and Ecology, Faculty of Biology, Adam Mickiewicz University, Poznań, Poland.

3.5. Integrative description of *Mesobiotus radiatus* population from Kenya

3.5.1. Animals (measurements and statistics in Table 3)

In live animals, body almost transparent in small specimens and white in adults; after fixation in Hoyer's medium body transparent (Figure 1A). Eyes absent (before fixation). Body cuticle without pores, smooth under PCM but under SEM very delicate granulation covering dorsolateral cuticle is visible (Figure 1B; granule diameter ranges from 0.04 to 0.08 µm and thus it is below PCM resolution). Granulation on legs I–IV present and visible both under PCM and SEM (granules 0.3–0.4 µm in diameter; Figures 2A, 2B, 2E, and 2F). A pulvinus-like cuticular bulge/fold is present on the internal surface of legs I–III (Figures 2C and 2D, filled arrowhead), whereas weakly marked muscle attachments are present just above the claws (Figures 2C and 2D, flat empty arrowhead). Both structures are visible only if the legs are fully extended and oriented on the slide.

Buccopharyngeal apparatus of the *Macrobiotus* type, with the ventral lamina and ten small peribuccal lamellae (Figure 3A). The oral cavity armature well developed and composed of three bands of teeth (Figures 3B, 3C, 4A, and 4B, arrowheads). The first band of teeth is composed of numerous extremely small cones arranged in four to six rows situated anteriorly in the oral cavity, just behind the bases of the peribuccal lamellae (Figures 3B, 3C, 4A, and 4B, filled arrowheads). The second band of teeth is situated between the ring fold and the third band of teeth and is composed of a number of small ridges parallel to the main axis of the buccal tube (Figures 3B, 3C, 4A, and 4B, empty arrowheads). The teeth of the third band are located within the posterior portion of the oral cavity, between the second
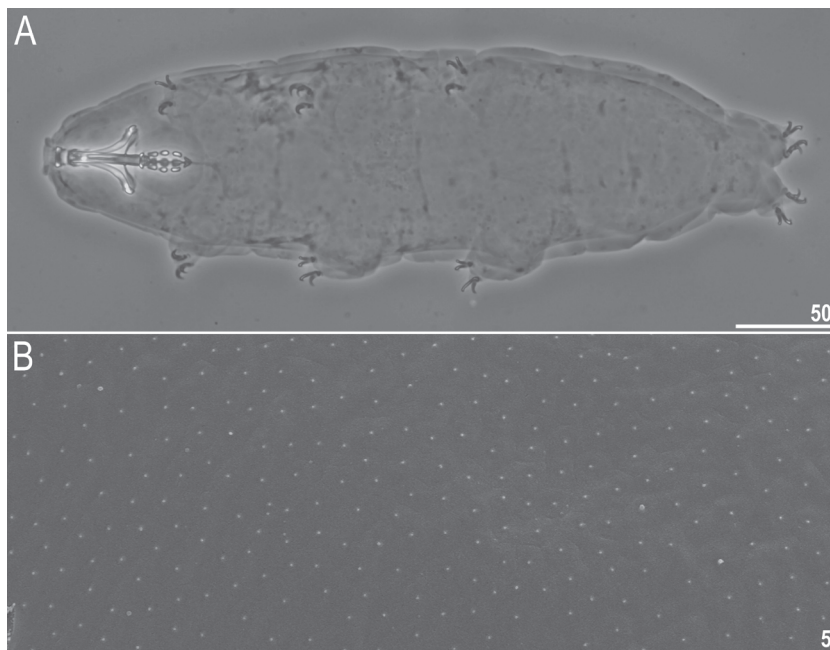

Figure 1. *Mesobiotus radiatus* (Pilato, Binda & Catanzaro, 1991) from Kenya – habitus and cuticle morphology: A) dorsoventral projection of the entire animal (Hoyer's medium, PCM); B) microgranulation on the dorsal cuticle seen in SEM. Scale bars in µm.

Figure 2. *Mesobiotus radiatus* (Pilato, Binda & Catanzaro, 1991) from Kenya – cuticular structures on legs: A, B) granulation on leg III seen in PCM and SEM, respectively; C, D) a pulvinus-like cuticular bulge on the internal surface of leg III seen in PCM and SEM, respectively; E, F) granulation on leg IV seen in PCM and SEM, respectively. Filled arrowheads indicate the cuticular bulge whereas empty arrowheads indicate faint muscle attachments under the claws. Scale bars in μm.
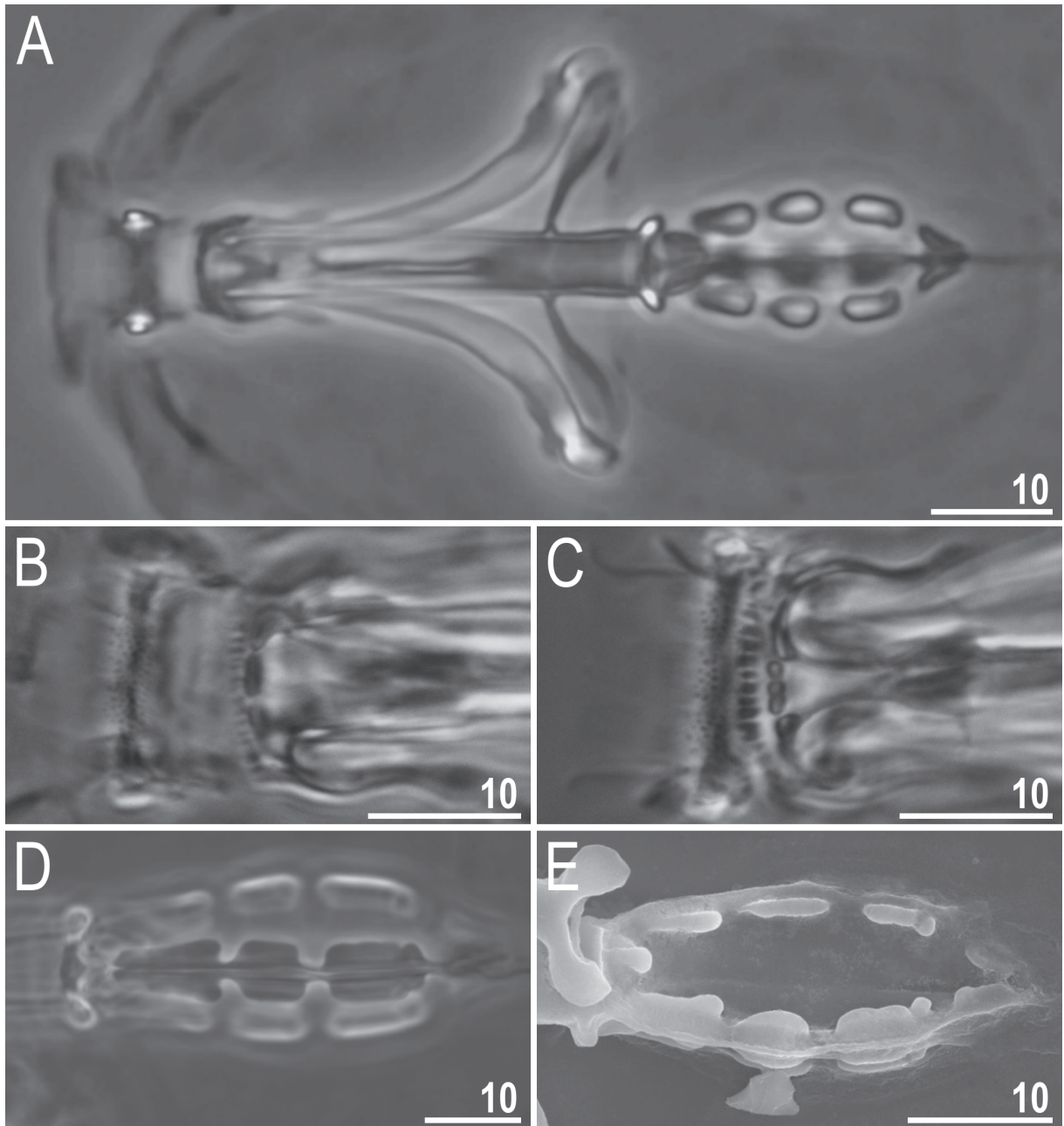
Figure 3. *Mesobiotus radiatus* (Pilato, Binda & Catanzaro, 1991) from Kenya – buccal apparatus and the oral cavity armature: A) dorsoventral projection of the entire buccal apparatus (PCM); B, C) oral cavity armature with all three bands of teeth visible, dorsal and ventral view respectively (PCM); D, E) placoid morphology seen in PCM and SEM, respectively. Scale bars in μm.

band of teeth and the buccal tube opening (Figures 3B, 3C, 4A, and 4B). The third band of teeth is discontinuous and divided into the dorsal and the ventral portion. Under PCM, the dorsal teeth are seen as three distinct transversal ridges/crests, whereas the ventral teeth appear as two separate lateral transversal ridges/crests between which three (only sometimes two or four) round median teeth are visible (Figures 3B and 3C). Also in SEM, both dorsal

and ventral teeth are clearly distinct (Figures 4A and 4B, lateral teeth labeled "L", dorsomedian tooth labeled "M", ventromedian teeth labeled "m_1–m_2"). Pharyngeal bulb spherical, with triangular apophyses, three rod-shaped macroplacoids, and a large triangular microplacoid (Figure 3A), with the macroplacoid length sequence of $2 < 1 \leq 3$. The first macroplacoid is anteriorly narrowed and the third has a subterminal constriction (Figures 3D and 3E).
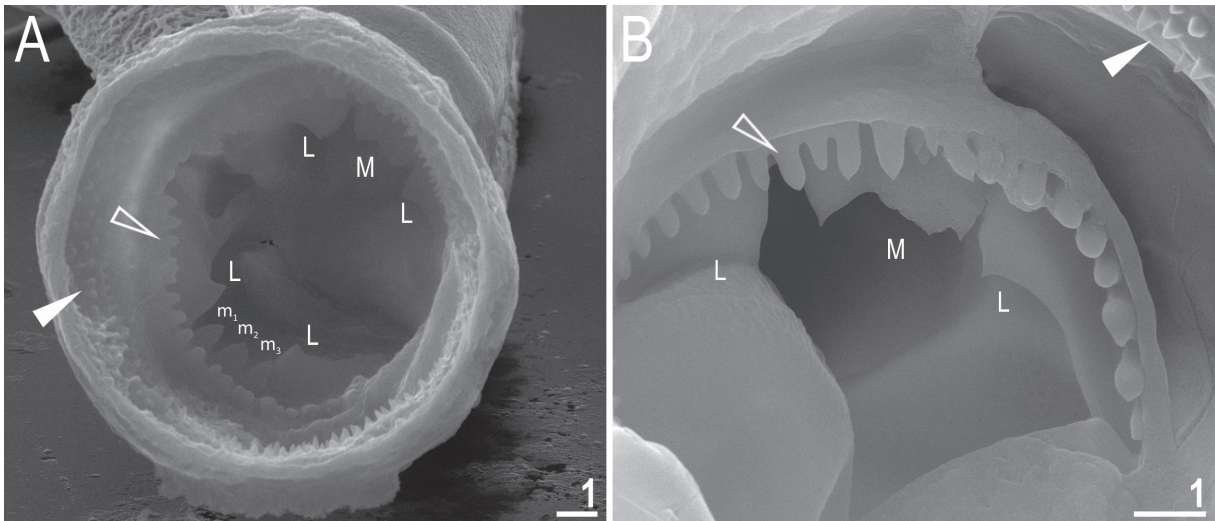
Figure 4. *Mesobiotus radiatus* (Pilato, Binda & Catanzaro, 1991) from Kenya – the oral cavity armature of two specimens seen in SEM: A) dorsal and ventral side; B) magnification on dorsal side. Filled indented arrowheads indicate teeth of the first band, empty indented arrowheads indicate teeth of the second band, the ridges of the third band are marked with "M" (dorsomedian tooth), "L" (lateral teeth, both dorsal and ventral), and "m_1–m_3" (ventromedian teeth). Scale bars in μm.

Claws of the *Mesobiotus* type, with a peduncle connecting the claw to the lunula, a basal septum, and well-developed accessory points situated on the primary branch (Figures 5A–5E). Lunulae under claws I–III smooth (Figures 5A and 5C), but dentate under claws IV (Figures 5B, 5D, 5E). Teeth on lunulae better developed under posterior than anterior claws (Figures 5D and 5E). Claws I–III often have short and very thin spurs at their bases, which are barely visible under PCM (Figure 5A, arrowhead) but better visible under SEM (Figure 5C, arrowhead)

3.5.2. Eggs (measurements and statistics in Table 4)
Laid freely, white, spherical with conical processes (Figures 6A–6D, 7A–7F, 8A–8D, and 9C–9F). The processes are equidistant from each other, with circular bases (Figures 6A–6D, 8A–8D, and 9C–9F). The process surface is smooth with slight undulations poorly visible under PCM and clearly under SEM (Figures 7A–7F, 8A–8D, and 9A–9F). The labyrinthine layer within the process walls appears as reticulation under PCM, with mesh size decreasing from bottom to top of the process (Figures 6E, 6F, and 7A–7F). Apical process wall porous, but pores (0.3–0.4 μm in diameter) poorly visible in PCM (Figure 7A–7C) and clearly visible in SEM (Figures 9C–9F and 10A–10E). Processes are terminated by several short, thin, and flexible filaments very susceptible to fracture, which are visible in both PCM (Figures 7A–7F) and SEM (Figures 8A–8D, 9C–9F, and 10A–10E). The filaments are covered by microgranules (0.1–0.2 μm in diameter; visible only in SEM), which probably enhance their adhesive properties. The processes are sometimes bi- or trifurcated

(Figures 7D–7F, 9D, and 10D). Egg surface between processes without areolation, but covered by wrinkles that extend radially from process bases (Figures 6E, 6F, 8A–8D, and 9A–9F). Small, round pores (0.3–0.5 μm in diameter) are present between the wrinkles and are usually visible in PCM and always clearly in SEM (Figures 6E, 6F, and 9A–9F).

The aceto-orcein staining revealed males with developed testes filled by spermatozoa. The population is thus dioecious, although no secondary sexual dimorphism characters (e.g., gibbosities on the hind legs) were observed.

3.6. DNA sequences
We obtained sequences of good quality for all four of the aforementioned molecular markers from all four paragenophores. The 18S rRNA and 28S rRNA sequences were represented by single haplotypes, whereas the ITS-2 and COI markers were represented by two haplotypes different in one variable site (p-distance: 0.3%) and four nucleotides (p-distance: 0.6%), respectively:

The 18S rRNA sequence (GenBank: MH197153), 865 bp long;

The 28S rRNA sequence (GenBank: MH197152), 736 bp long;

The ITS-2 sequence, haplotype 1 (GenBank: MH197267), 390 bp long;

The ITS-2 sequence, haplotype 2 (GenBank: MH197268), 390 bp long;

The COI sequence, haplotype 1 (GenBank: MH195147), 658 bp long;

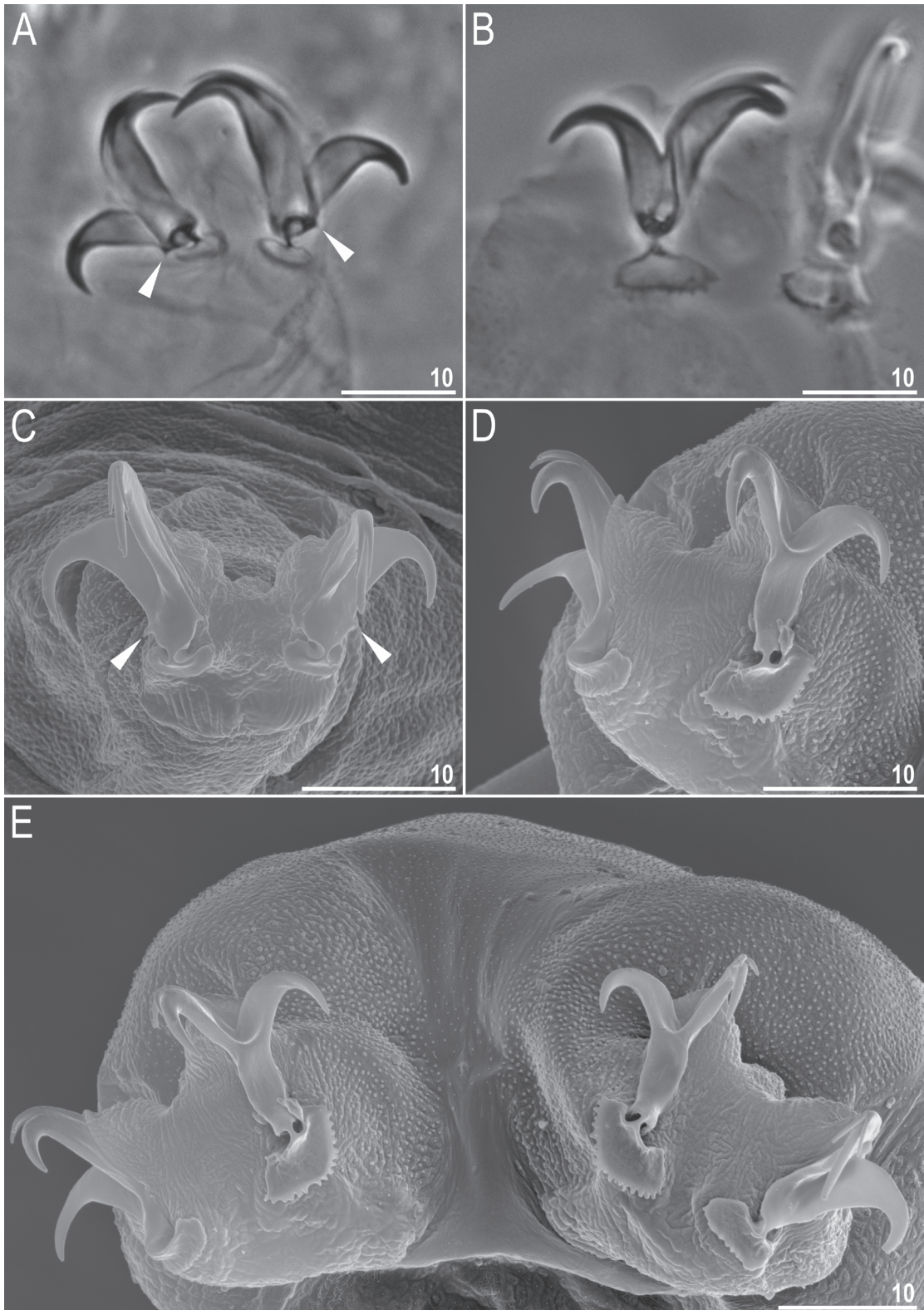The COI sequence, haplotype 2 (GenBank: MH195148), 658 bp long.

Figure 5. *Mesobiotus radiatus* (Pilato, Binda & Catanzaro, 1991) from Kenya – claws: A, B) claws I and IV seen in PCM, with smooth and dentate lunulae, respectively; C, D) claws II and IV seen in SEM, with smooth and dentate lunulae, respectively; E) the overall view of the hind legs, note better developed teeth on lunulae under posterior claws and granulation morphology; arrowheads indicate spurs at the claw bases. Figures A and B assembled from several photos. Scale bars in μm.

Table 4. Measurements [in μm] of selected morphological structures of the eggs of *Mesobiotus radiatus* (Pilato, Binda & Catanzaro, 1991) from Kenya mounted in Hoyer's medium (N: number of eggs/structures measured, Range: smallest and the largest structures among all measured specimens; SD: standard deviation).

Character	N	Range	Mean	SD
Egg bare diameter	30	63.9–80.4	72.6	4.4
Egg full diameter	30	97.8–131.1	114.4	8.3
Process height	90	15.5–29.3	21.6	3.1
Process base width	90	14.5–22.5	17.3	1.6
Process base/height ratio	90	63%–118%	81%	13%
Distance between processes	90	2.1–7.1	4.0	1.0
Number of processes on the egg circumference	30	10–12	11.1	0.5

4. Discussion

4.1. Comparison with the original description

Our observations are in line with those presented in the original description of *M. radiatus* (Pilato et al., 1991). However, thanks to the use of high class PCM and SEM, we were able to describe some new traits that were not described by Pilato et al. (1991). Specifically, SEM observations revealed small, cuticular granulation on the entire dorsolateral cuticle (not visible in PCM), whereas under both microscopes short and very thin spurs at claw bases I–III were discovered. Our observations of eggs in PCM and SEM revealed small, round pores between the wrinkles on the egg surface, larger pores in the apical process wall, and several short, thin, and flexible filaments on the process apex. Moreover, thanks to the larger sample size, we were able to estimate intraspecific variation in taxonomically important traits of both animals and eggs more accurately. In conclusion, we think that, by adding new data to the original description of the species by Pilato et al. (1991), our study will be helpful for future species identification and discoveries.

4.2. New phenotypic differential diagnosis

Based on the presence of reticulated conical egg processes and wrinkled egg surface, *M. radiatus* is most similar to the following ten *Mesobiotus* species: *M. binieki* (Kaczmarek, Gołdyn, Prokop & Michalczyk, 2011); *M. coronatus* (de Barros, 1942); *M. patiens* (Pilato, Binda, Napolitano & Moncada, 2000); *M. perfidus* (Pilato & Lisi, 2009); *M. philippinicus* Mapalo, Stec, Mirano-Bascos & Michalczyk, 2016; *M. pseudocoronatus* (Pilato, Binda & Lisi, 2006); *M. pseudopatiens* Kaczmarek & Roszkowska, 2016; *M. rigidus* (Pilato & Lisi, 2006); *M. simulans* (Pilato, Binda, Napolitano & Moncada, 2000); and *M. wuzhishanensis* (Yin, L. Wang & X. Li, 2011). Despite the similarities, *M. radiatus* differs specifically from:

· **M. binieki**, reported only from its type locality in Bulgaria (Kaczmarek et al., 2011), by indentations in lunulae IV; a different shape of egg processes (typically developed cones in *M. radiatus* vs. long, smooth flexible spines with very wide bases in *M. binieki*); the presence of several apical short, thin, and flexible filaments on egg processes; smaller egg bare diameter (63.9–80.4 μm in *M. radiatus* vs. 85.1–94.5 μm in *M. binieki*); longer egg processes (15.5–29.3 μm in *M. radiatus* vs. 9.8–14.5 μm in *M. binieki*); wider egg process bases (14.5–22.5 μm in *M. radiatus* vs. 6.5–9.0 μm in *M. binieki*); and a smaller number of processes on the egg circumference (10–12 in *M. radiatus* vs. 27–32 in *M. binieki*).

· **M. coronatus**, known from a few localities in South America (see Kaczmarek et al., 2015), by indentations in lunulae IV; the absence of eyes; the presence of apical short, thin, and flexible filaments on egg processes; radially arranged wrinkles on the egg surface between processes (wrinkles forming a sculpture with fine polygonal meshes in *M. coronatus*); larger egg bare and full diameters (63.9–80.4 μm and 97.8–131.1 μm in *M. radiatus* vs. 42.0–55.0 μm and 55.0–71.0 μm in *M. coronatus*); longer egg processes (15.5–29.3 μm in *M. radiatus* vs. ca. 9.2 μm in *M. coronatus*); and wider egg process bases (14.5–22.5 μm in *M. radiatus* vs. 9.6–10.4 μm in *M. coronatus*).

· **M. patiens**, recorded from a few localities in Italy (Pilato et al., 2000), by indentations in lunulae IV; the presence of several apical short, thin, and flexible filaments on egg processes; and radially arranged wrinkles on the egg surface between processes (fine in *M. patiens*).

· **M. perfidus**, known from three localities in the Seychelles (Pilato and Lisi, 2009), by the presence of the first band of teeth in the oral cavity; the absence of tubercles on the dorsal cuticle; indentations in lunula IV; the absence of eyes; and the presence of several apical short, thin, and flexible filaments on egg processes.
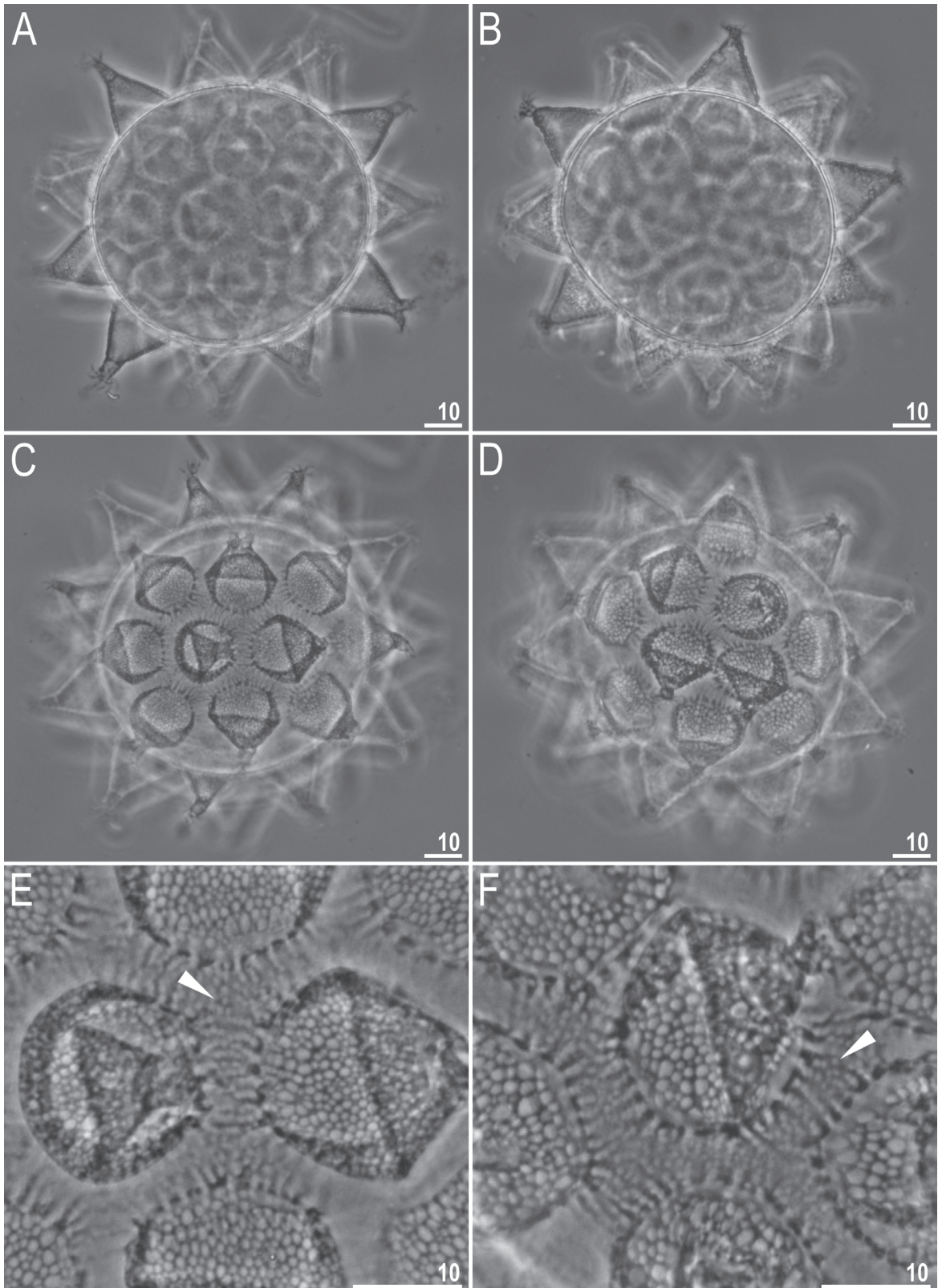
Figure 6. *Mesobiotus radiatus* (Pilato, Binda & Catanzaro, 1991) from Kenya – egg seen in PCM: A, B) midsection under 400× magnification; C, D) surface under 400× magnification; E, F) surfaces under 1000× magnification. Photos of each column show the details of a single egg. Arrowheads indicate pores on the egg surface between processes. Scale bars in μm.
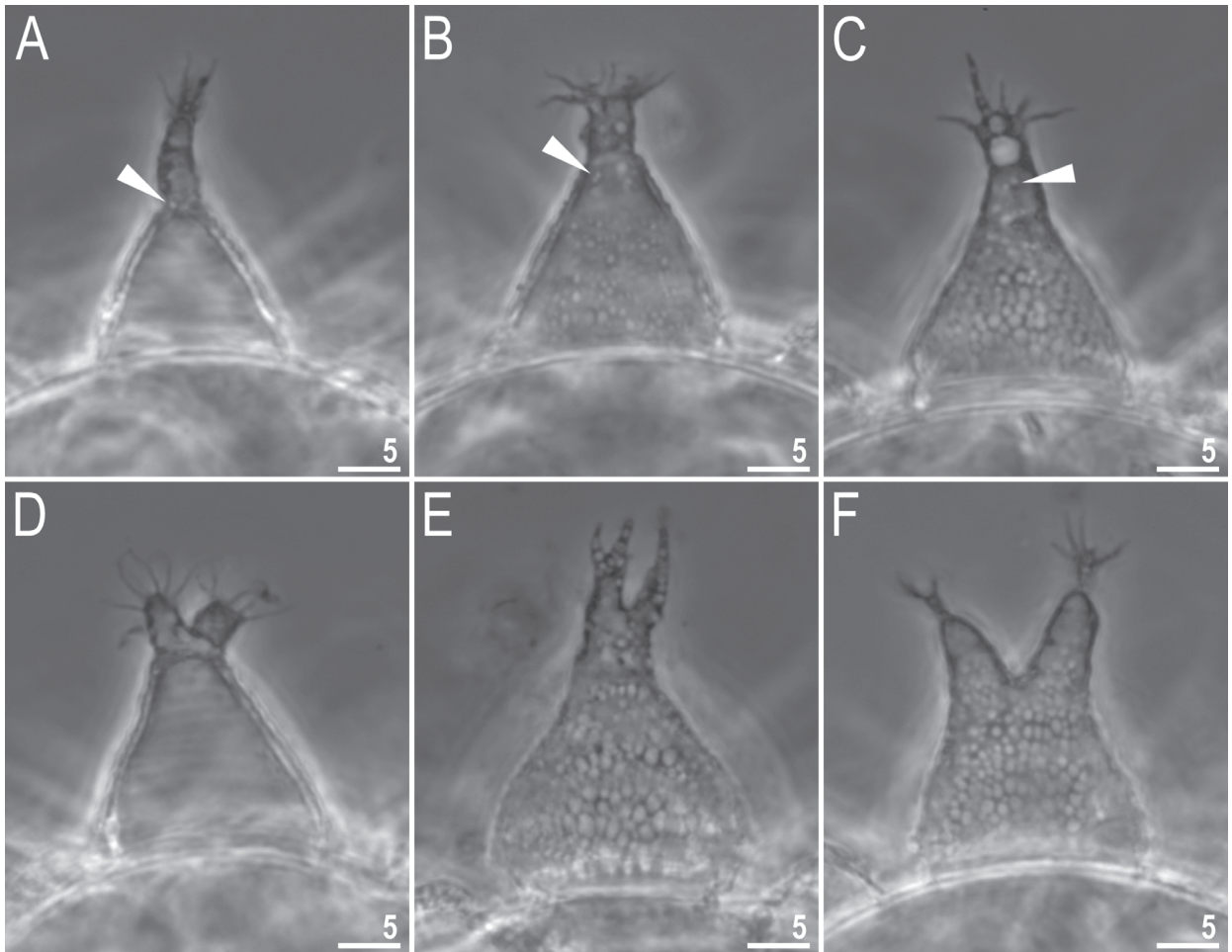
Figure 7. *Mesobiotus radiatus* (Pilato, Binda & Catanzaro, 1991) from Kenya – egg processes seen in PCM under 1000× magnification. Photos of several eggs. Arrowheads indicate pores in the apical process wall. Scale bars in µm.

· ***M. philippinicus***, reported from the type locality in the Philippines (Mapalo et al., 2016), by a different macroplacoid length sequence (2 < 1 ≤ 3 in *M. radiatus* vs. 2 < 3 < 1 in *M. philippinicus*); the presence of pores in the apical wall of egg processes (visible in SEM only); larger egg full diameter (97.8–131.1 µm in *M. radiatus* vs. 71.4–97.5 µm in *M. philippinicus*); longer egg processes (15.5–29.3 µm in *M. radiatus* vs. 2.1–13.7 µm in in *M. philippinicus*); wider egg process bases (14.5–22.5 µm in *M. radiatus* vs. 7.1–13.0 µm in *M. philippinicus*); and a smaller number of processes on egg circumference (10–12 in *M. radiatus* vs. 15–17 in *M. philippinicus*).

· ***M. pseudocoronatus***, recorded from the type locality in the Seychelles (Pilato et al., 2006), by the absence of tubercles on the dorsal cuticle; the absence of eyes; longer egg processes (15.5–29.3 µm in *M. radiatus* vs. 10.9–12.7 µm in *M. pseudocoronatus*); and wider egg process bases (14.5–22.5 µm in *M. radiatus* vs. 11.5–13.9 µm in *M. pseudocoronatus*).

· ***M. pseudopatiens***, known from the type locality in Costa Rica (Kaczmarek and Roszkowska, 2016), by the presence of the first row of teeth in the oral cavity; the presence of granulation on legs I–III; indentations in lunulae IV; and larger bare and full egg diameters (63.9–80.4 µm and 97.8–131.1 µm in *M. radiatus* vs. 55.5–59.3 µm and 80.4–88.0 µm in *M. pseudopatiens*).

· ***M. rigidus***, reported from the type locality in New Zealand (Pilato and Lisi, 2006), by indentations in lunulae IV; a different shape of egg processes (cones in *M. radiatus* vs. long, smooth flexible spines, with very wide bases in *M. rigidus*); and the presence of several apical short, thin, and flexible filaments on egg processes.

· ***M. simulans***, known from a few localities in Italy (Pilato et al., 2000), by the absence of eyes; presence of several apical short, thin, and flexible filaments on egg processes; radially arranged wrinkles on the egg surface between processes (wrinkles forming a sculpture with
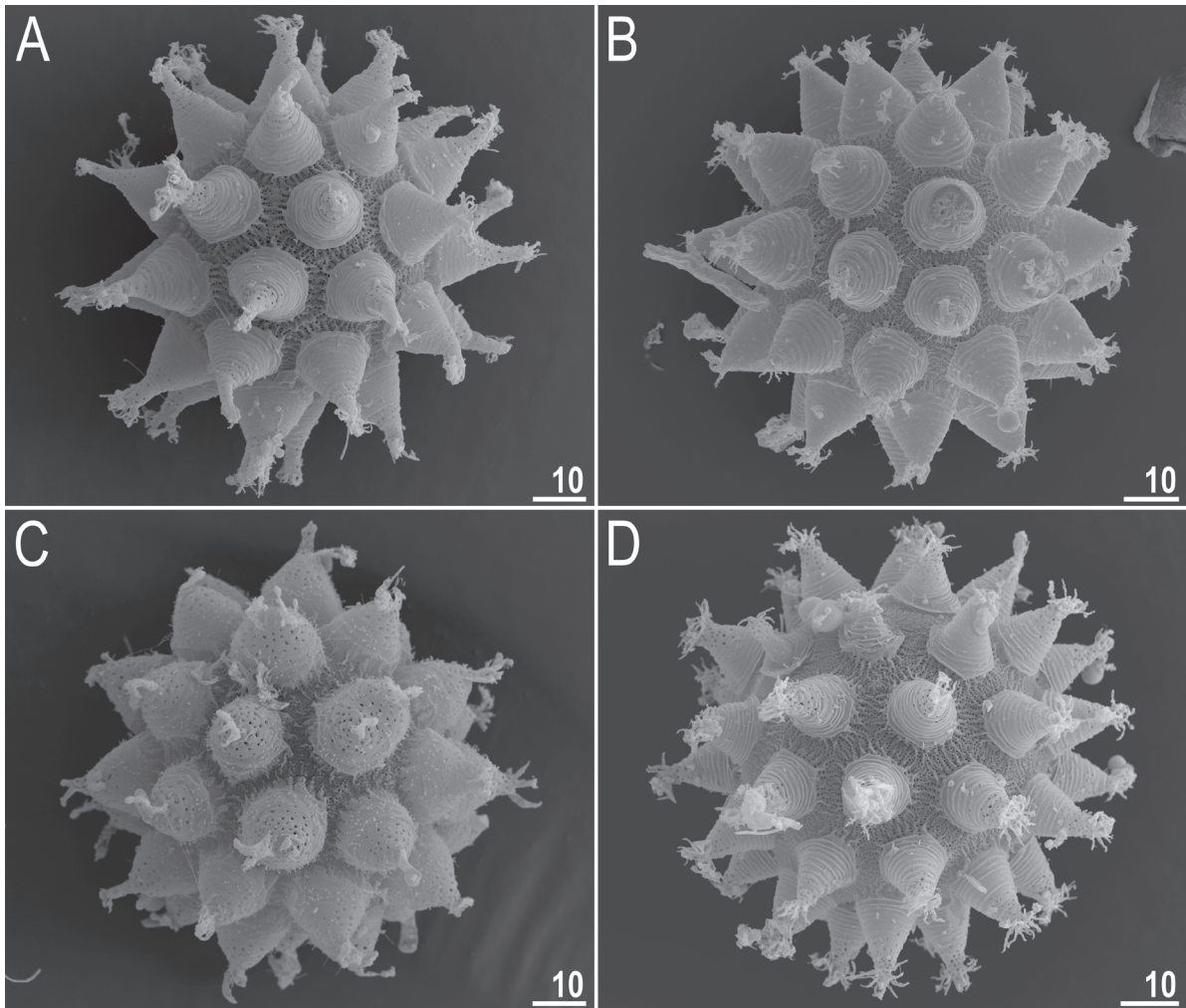
Figure 8. *Mesobiotus radiatus* (Pilato, Binda & Catanzaro, 1991) from Kenya – entire eggs seen in SEM. Scale bars in μm.

fine polygonal meshes in *M. simulans*); longer egg processes (15.5–29.3 μm in *M. radiatus* vs. max. 11.0 μm in *M. simulans*); and wider egg process bases (14.5–22.5 μm in *M. radiatus* vs. 11.0–14.0 μm in *M. simulans*).

· **M. wuzhishanensis**, recorded from the type locality in China (Yin et al., 2011), by the absence of eyes; a different shape of egg processes (cones in *M. radiatus* vs. long, smooth flexible spines, with very wide bases in *M. wuzhishanensis*); and a smaller number of processes on the egg circumference (10–12 in *M. radiatus* vs. ca. 16 in *M. wuzhishanensis*).

4.3. Genotypic differential diagnosis
The ranges of uncorrected genetic p-distances between the studied population of *Mesobiotus radiatus* and species of the genus *Mesobiotus* for which sequences are available from GenBank (see Table 2 for details) are as follows:

· **18S rRNA**: 0.5%–5.6% (3.8% on average), with the most similar being *M. ethiopicus* from Ethiopia

(MF678793) and the least similar being *M.* cf. *mottai* from Antarctica (KT226072).

· **28S rRNA**: 4.0%–9.0% (7.3% on average), with the most similar being *M. ethiopicus* from Ethiopia (MF678792) and the least similar being *M. philippinicus* and *M. insanis* from the Philippines (KX129794, MF441489, respectively).

· **ITS-2**: 28.7%–30.5% (29.6% on average), with the most similar being *M. insanis* from the Philippines (MF441490) and the least similar *M. philippinicus* from the Philippines (KX129795).

· **COI**: 16.5%–25.2% (22.1% on average), with the most similar being *M. ethiopicus* from Ethiopia (MF678794) and the least similar being *M. philippinicus* from the Philippines (KX129796).

4.4. Closing remarks
Although our individuals and eggs fit the description of *M. radiatus* well and they were collected in the same ecozone and ca. 670 km from the type locality of the species, there
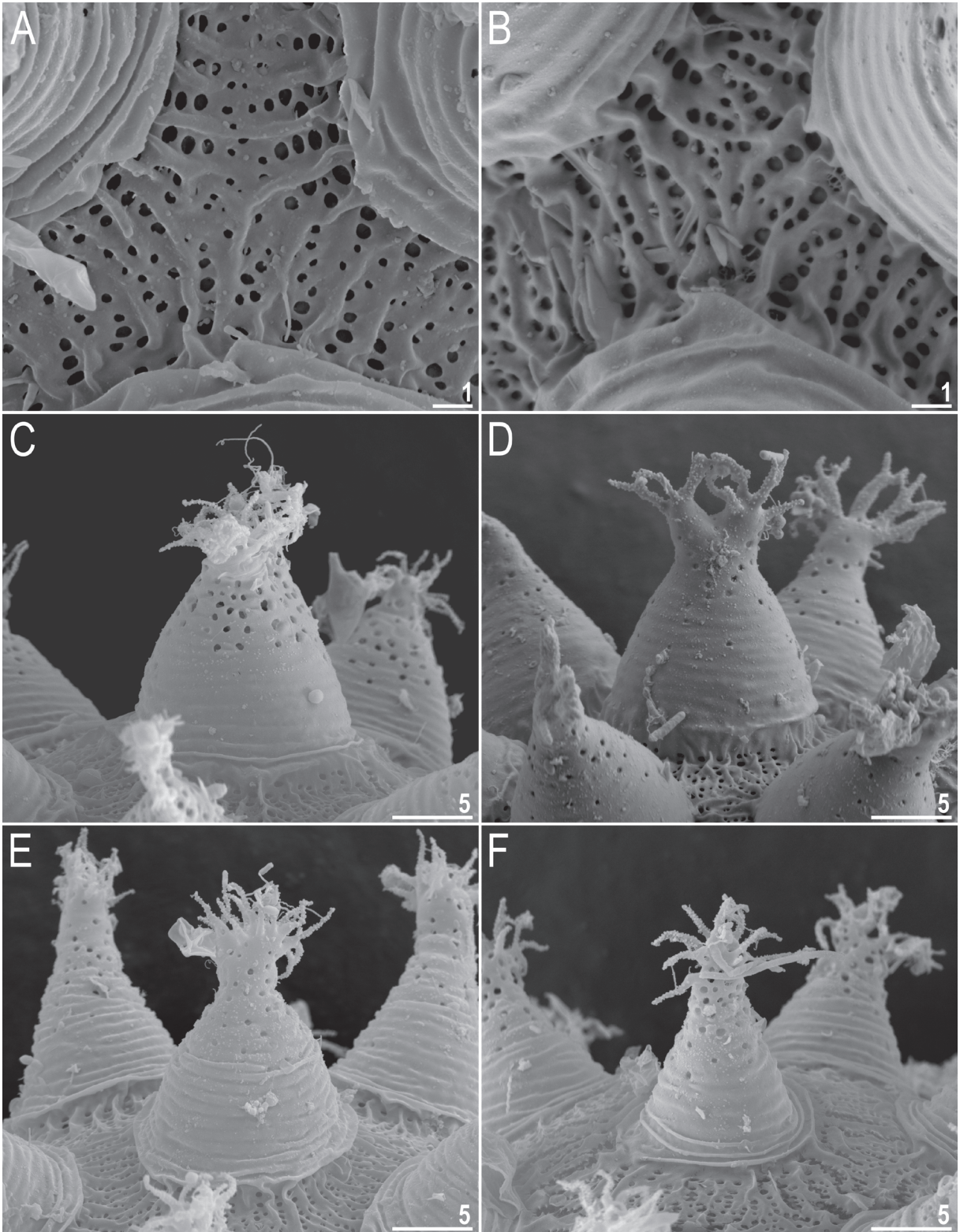
Figure 9. *Mesobiotus radiatus* (Pilato, Binda & Catanzaro, 1991) from Kenya – details of eggs seen in SEM: A, B) – egg surface between processes; C–F) egg processes morphology. Scale bars in μm.
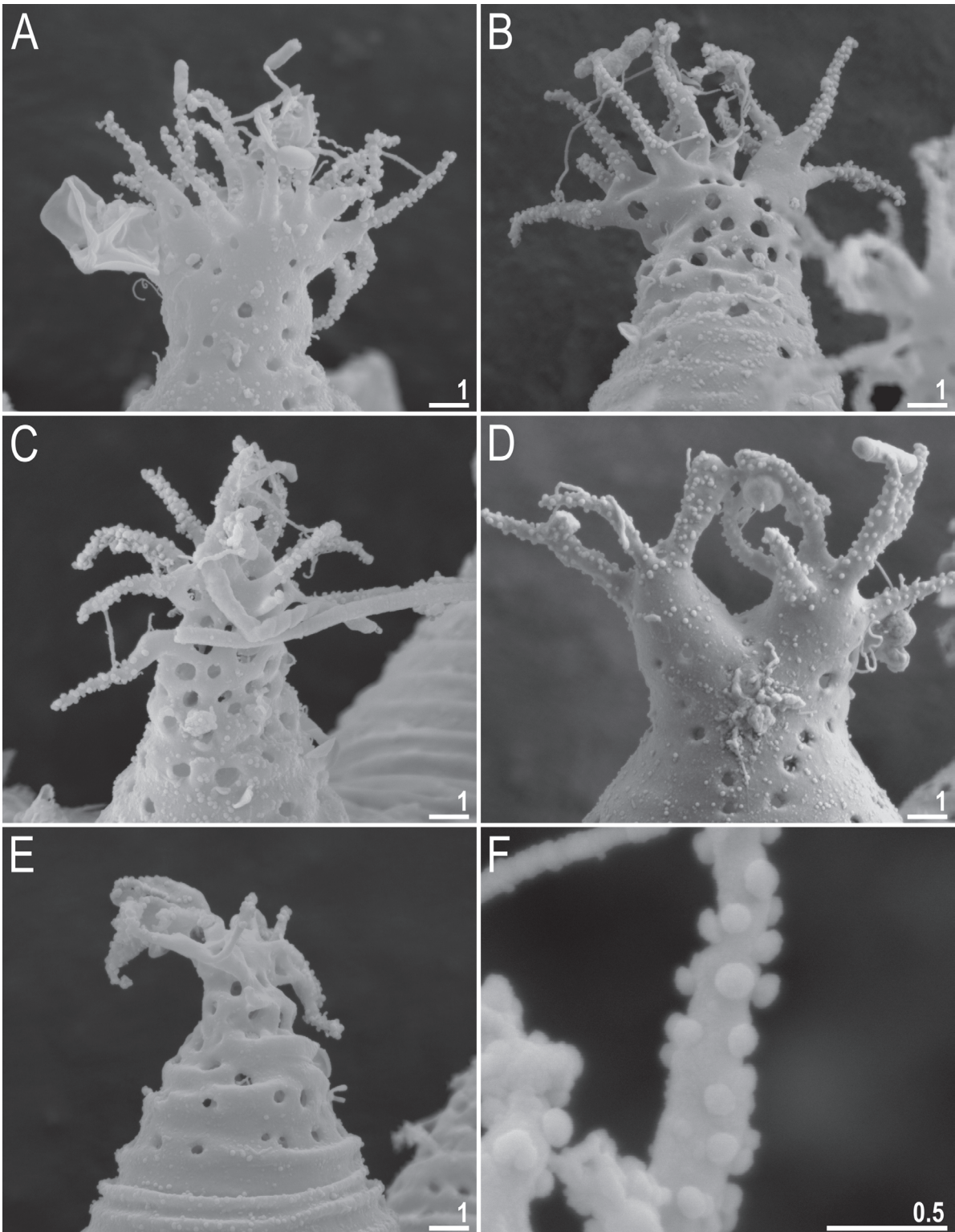
Figure 10. *Mesobiotus radiatus* (Pilato, Binda & Catanzaro, 1991) from Kenya – details of eggs seen in SEM: A–E) porous apices of egg processes with short flexible filaments; F) magnification of flexible filament. Scale bars in μm.

is a possibility that the Kenyan population represents a different but very similar or cryptic species. On the other hand, several tardigrade species were shown, with the use of genetic markers, to have distributions exceeding the distance between the type population and the Kenyan population of M. radiatus (Jørgensen et al., 2017; Gąsiorek et al., 2016, Zawierucha et al., 2018, Gąsiorek et al., in press, Morek et. al., in press). Therefore, until DNA sequences for a population of *M. radiatus* from the type locality are obtained and they confirm our identification of the Kenyan population, this integrative description of *M. radiatus* must be treated with a small dose of caution.

References

Bertolani R, Guidetti R, Marchioro T, Altiero T, Rebecchi L, Cesari M (2014). Phylogeny of Eutardigrada: new molecular data and their morphological support lead to the identification of new evolutionary lineages. Mol Phylogenet Evol 76: 110-126.

Binda MG, Pilato G, Moncada E, Napolitano A (2001). Some tardigrades from Central Africa with the description of two new species: *Macrobiotus ragonesei* and *M. priviterae* (Eutardigrada: Macrobiotidae). Trop Zool 14: 233-242.

Casquet J, Thebaud C, Gillespie RG (2012). Chelex without boiling, a rapid and easy technique to obtain stable amplifiable DNA from small amounts of ethanol-stored spiders. Mol Ecol Resour 12: 136-141.

Dastych H (1980). Niesporczaki (Tardigrada) Tatrzańskiego Parku Narodowego. Monografie Fauny Polski 9: 1-232 (in Polish).

Dayrat B (2005). Towards integrative taxonomy. Biol J Linnean Soc 85: 407-415.

de Barros R (1942). Tardigrados de Estado de Sao Paulo, Brasil. II. Gênero *Macrobiotus*. Rev Brasil Biol 2: 373-386 (in Portuguese).

Degma P, Bertolani R, Guidetti R 34: (2009-2018). Actual checklist of Tardigrada species (30-06-2018). Available online at www.evozoo.unimore.it/site/home/documento1080026927.html.

Degma P, Guidetti R (2007). Notes to the current checklist of Tardigrada. Zootaxa 1579: 41-53.

Doyère LMF (1840). Memoire sur les Tardigrades. I. Ann Sci Nat Paris Series 2 14: 269-362 (in French).

Eibye-Jacobsen J (2001). A new method for making SEM preparations of the tardigrade buccopharyngeal apparatus. Zool Anz 240: 309-319.

Folmer O, Black M, Hoeh W, Lutz R, Vrijenhoek R (1994). DNA primers for amplification of mitochondrial cytochrome c oxidase subunit I from diverse metazoan invertebrates. Mol Mar Biol Biotechnol 3: 294-299.

Fontoura P, Lisi O, Pilato G (2013). A new tardigrade *Doryphoribius maasaimarensis* sp. nov. (Eutardigrada: Hypsibiidae) from Kenya. Zootaxa 3630: 359-368.

Gąsiorek P, Stec D, Morek W, Michalczyk Ł (2017). An integrative redescription of *Echiniscus testudo* (Doyère, 1840), the nominal taxon for the class Heterotardigrada (Ecdysozoa: Panarthropoda: Tardigrada). Zool Anz 270: 107-122.

Gąsiorek P, Stec D, Morek W, Zawierucha K, Kaczmarek Ł, Lachowska-Cierlik D, Michalczyk Ł (2016). An integrative revision of *Mesocrista* Pilato, 1987 (Tardigrada: Eutardigrada: Hypsibiidae). J Nat Hist 50: 2803-2828.

Gąsiorek P, Vončina K, Michalczyk Ł (in press) *Echiniscus testudo* (Doyère, 1840) in New Zealand: anthropogenic dispersal or evidence for the "Everything is Everywhere" hypothesis? New Zeal J Zool.

Guidetti R, Bertolani R (2005). Tardigrade taxonomy: an updated check list of the taxa and a list of characters for their identification. Zootaxa 845: 1-46.

Guidetti R, Schill RO, Bertolani R, Dandekar T, Wolf M (2009). New molecular data for tardigrade phylogeny, with the erection of *Paramacrobiotus* gen. nov. J Zool Syst Evol Res 47: 315-321.

Hall TA (1999). BioEdit: A user-friendly biological sequence alignment editor and analysis program for Windows 95/98/NT. Nucleic Acids Symp Ser 41: 95-98.

Hebert PDN, Cywinska A, Ball SL, deWaard JR (2003). Biological identifications through DNA barcodes. Proc R Soc London Ser B Biol Sc 270: 313-322.

Jørgensen A, Mobjerg N, Kristensen RM (2007). A molecular study of the tardigrade *Echiniscus testudo* (Echiniscidae) reveals low DNA sequence diversity over a large geographical area. J Limnol 66 (Suppl. 1): 77-83.

Kaczmarek Ł, Cytan J, Zawierucha K, Diduszko D, Michalczyk Ł (2014). Tardigrades from Peru (South America), with descriptions of three new species of Parachela. Zootaxa 3790: 357-379.

Kaczmarek Ł, Gołdyn B, Prokop ZM, Michalczyk Ł (2011). New records of Tardigrada from Bulgaria with the description of *Macrobiotus binieki* sp. nov. (Eutardigrada: Macrobiotidae) and a key to the species of the *harmsworthi* group. Zootaxa 2781: 29-39.

Kaczmarek Ł, Michalczyk Ł (2017). The *Macrobiotus hufelandi* (Tardigrada) group revisited. Zootaxa 4363: 101-123.

Kaczmarek Ł, Michalczyk Ł, McInnes SJ (2015). Annotated zoogeography of non-marine Tardigrada. Part II: South America. Zootaxa 3923: 1-107.

Kaczmarek Ł, Roszkowska M (2016). A new eutardigrade from Costa Rica with taxonomical and zoogeographical remarks on Costa Rican tardigrades. New Zeal J Zool 43: 234-245.

Katoh K, Misawa K, Kuma K, Miyata T (2002). MAFFT: A novel method for rapid multiple sequence alignment based on fast Fourier transform. Nucleic Acids Res 30: 3059-3066.

Katoh K, Toh H (2008). Recent developments in the MAFFT multiple sequence alignment program. Brief Bioinform 9: 286-298.

Kumar S, Stecher G, Tamura K (2016). MEGA7: Molecular Evolutionary Genetics Analysis version 7.0 for bigger datasets. Mol Biol Evol 33: 1870-1874.

Mapalo M, Stec D, Mirano-Bascos DM, Michalczyk Ł (2016). *Mesobiotus philippinicus* sp. nov., the first limnoterrestrial tardigrade from the Philippines. Zootaxa 4126: 411-426.

Mapalo M, Stec D, Mirano-Bascos DM, Michalczyk Ł (2017). An integrative description of a limnoterrestrial tardigrade from the Philippines, *Mesobiotus insanis*, new species (Eutardigrada: Macrobiotidae: *harmsworthi* group). Raffles Bull Zool 65: 440-454.

Marley NJ, McInnes SJ, Sands CJ (2011). Phylum Tardigrada: A re-evaluation of the Parachela. Zootaxa 2819: 51-64.

McInnes SJ (1994). Zoogeographic distribution of terrestrial/freshwater tardigrades from current literature. J Nat Hist 28: 257-352.

McInnes SJ, Michalczyk Ł, Kaczmarek Ł (2017). Annotated zoogeography of non-marine Tardigrada. Part IV: Africa. Zootaxa 4284: 1-7.

Michalczyk Ł, Kaczmarek Ł (2003). A description of the new tardigrade *Macrobiotus reinhardti* (Eutardigrada, Macrobiotidae, *harmsworthi* group) with some remarks on the oral cavity armature within the genus *Macrobiotus* Schultze. Zootaxa 331: 1-24.

Michalczyk Ł, Kaczmarek Ł (2013). The Tardigrada Register: a comprehensive online data repository for tardigrade taxonomy. J Limnol 72: 175-181.

Michalczyk Ł, Wełnicz W, Frohme M, Kaczmarek Ł (2012). Redescriptions of three *Milnesium* Doyère, 1840 taxa (Tardigrada: Eutardigrada: Milnesiidae), including the nominal species for the genus. Zootaxa 3154: 1-20.

Mironov SV, Dabert J, Dabert M (2012). A new feather mite species of the genus *Proctophyllodes* Robin, 1877 (Astigmata: Proctophyllodidae) from the Long-tailed Tit *Aegithaloscaudatus* (Passeriformes: Aegithalidae): morphological description with DNA barcode data. Zootaxa 3253: 54-61.

Morek W, Stec D, Gąsiorek P, Schill RO, Kaczmarek Ł, Michalczyk Ł (2016). An experimental test of eutardigrade preparation methods for light microscopy. Zool J Linn Soc-Lond 178: 785-793.

Morek W, Stec D, Gąsiorek P, Surmacz B, Michalczyk Ł (in press). *Milnesium tardigradum* Doyère, 1840: the first integrative study of inter-population variability in a tardigrade species. J Zool Syst Evol Res.

Murray J (1910). Tardigrada. British Antarctic Expedition 1907–1909. Reports on the Scientific Investigations. Vol. 1 Biology (Part V). London, UK: W. Heinemann.

Murray J (1913). African Tardigrada. J R Micr Soc London 2: 136-144.

Nelson DR, Guidetti R, Rebecchi L (2015). Phylum Tardigrada. In: Thorp J, Rogers DC, editors. Ecology and General Biology: Vol. 1: Thorp and Covich's Freshwater Invertebrates. 4th Revised Edition. Amsterdam, the Netherlands: Academic Press, pp. 347-380.

Pilato G (1981). Analisi di nuovi caratteri nello studio degli Eutardigrada. Animalia 8: 51-57 (in Italian).

Pilato G, Binda MG (2010). Definition of families, subfamilies, genera and subgenera of the Eutardigrada, and keys to their identification. Zootaxa 2404: 1-52.

Pilato G, Binda MG, Catanzaro R (1991). Remarks on some tardigrades of the African fauna with the description of three new species of *Macrobiotus* Schultze 1834. Trop Zool 4: 167-178.

Pilato G, Binda MG, Lisi O (2006). Eutardigrada from New Zealand, with descriptions of two new species. New Zeal J Zool 33: 49-63.

Pilato G, Binda MG, Napolitano A, Moncada E (2000). The specific value of *Macrobiotus coronatus* DeBarros 1942, and description of two new species of the *harmsworthi* group (Eutardigrada). Boll Acc Gioenia Sci Nat 33: 103-120.

Pilato G, Lisi O (2006). *Macrobiotus rigidus* sp. nov., a new species of eutardigrade from New Zealand. Zootaxa, 1109: 49-55.

Pilato G, Lisi O (2009). Description of three new species of Tardigrada from the Seychelles. Zootaxa 2005: 24-34.

Richters F (1926). Tardigrada. In: Kükenthal W, Krumbach T, editors. Handbuch der Zoologie Vol. 3. Berlin, Germany: Walter de Gruyter & Co., pp. 58-61 (in German).

Schill RO, Forster F, Dandekar T, Wolf N (2010). Using compensatory base change analysis of internal transcribed spacer 2 secondary structures to identify three new species in *Paramacrobiotus* (Tardigrada). Org Divers Evol 10: 287-296.

Schultze CAS (1834). *Macrobiotus Hufelandii* animal e crustaceorum classe novum, reviviscendi post diuturnam asphixiam et aridiatem potens, etc. 8, 1 tab. Berlin, Germany: C. Curths (in Latin).

Schultze CAS (1840). *Echiniscus Bellermanni*, Animal Crustaceum, *Macrobiotus Hufelandii* Affine. Berlin, Germany: Apud G. Reimer (in Latin).

Schuster RO, Nelson DR, Grigarick AA, Christenberry D (1980). Systematic criteria of the Eutardigrada. T Am Microsc Soc 99: 284-303.

Srivathsan A, Meier R (2012). On the inappropriate use of Kimura-2-parameter (K2P) divergences in the DNA-barcoding literature. Cladistics 28: 190-194.

Stec D, Gąsiorek P, Morek W, Kosztyła P, Zawierucha K, Michno K, Kaczmarek Ł, Prokop ZM, Michalczyk Ł (2016a). Estimating optimal sample size for tardigrade morphometry. Zool J Linn Soc-Lond 178: 776-784.

Stec D, Kristensen RM (2017). An integrative description of *Mesobiotus ethiopicus* sp. nov. (Tardigrada: Eutardigrada: Parachela: Macrobiotidae: *harmsworthi* group) from the Northern Afrotropic region. Turk J Zool 41: 800-811.

Stec D, Morek W, Gąsiorek P, Kaczmarek Ł, Michalczyk Ł (2016b). Determinants and taxonomic consequences of extreme egg shell variability in *Ramazzottius subanomalus* (Biserov, 1985) (Tardigrada). Zootaxa 4208: 176-188.

Stec D, Morek W, Gąsiorek P, Michalczyk Ł (2018). Unmasking hidden species diversity within the *Ramazzottius oberhaeuseri* complex, with an integrative redescription of the nominal species for the family Ramazzottiidae (Tardigrada: Eutardigrada: Parachela). Syst Biodivers 16: 357-376.

Stec D, Smolak R, Kaczmarek Ł, Michalczyk Ł (2015). An integrative description of *Macrobiotus paulinae* sp. nov. (Tardigrada: Eutardigrada: Macrobiotidae: *hufelandi* group) from Kenya. Zootaxa 4052: 501-526.

Stec D, Zawierucha K, Michalczyk Ł (2017). An integrative description of *Ramazzottius subanomalus* (Biserov, 1985) (Tardigrada) from Poland. Zootaxa 4300: 403-420.

Thulin G (1928). Über die Phylogenie und das System der Tardigraden. Hereditas 11: 207-266 (in German).

Vecchi M, Cesari M, Bertolani R, Jönsson KI, Rebecchi L, Guidetti R (2016). Integrative systematic studies on tardigrades from Antarctica identify new genera and new species within Macrobiotoidea and Echiniscoidea. Invertebr Syst 30: 303-322.

Yin H, Wang LH, Li XC (2011). Two new species of genus *Macrobiotus* (Tardigrada: Macrobiotidae) from China. Proc Biol Soc Wash 124: 165-178.

Zawierucha Z, Stec, D, Lachowska-Cierlik D, Takeuchi N, Li Z, Michalczyk Ł (2018) High mitochondrial diversity in a new water bear species (Tardigrada: Eutardigrada) from mountain glaciers in central Asia, with the erection of a new genus *Cryoconicus*. Ann Zool 68: 179-201.

Zeller C (2010). Untersuchung der Phylogenie von Tardigraden anhand der Genabschnitte 18S rDNA und Cytochrom c Oxidase Untereinheit 1 (COX I). MSc, Technische Hochschule Wildau, Wildau, Germany (in German).